Dalton Transactions

Accepted Manuscript

ROYAL SOCIETY OF CHEMISTRY

www.rsc.org/dalton

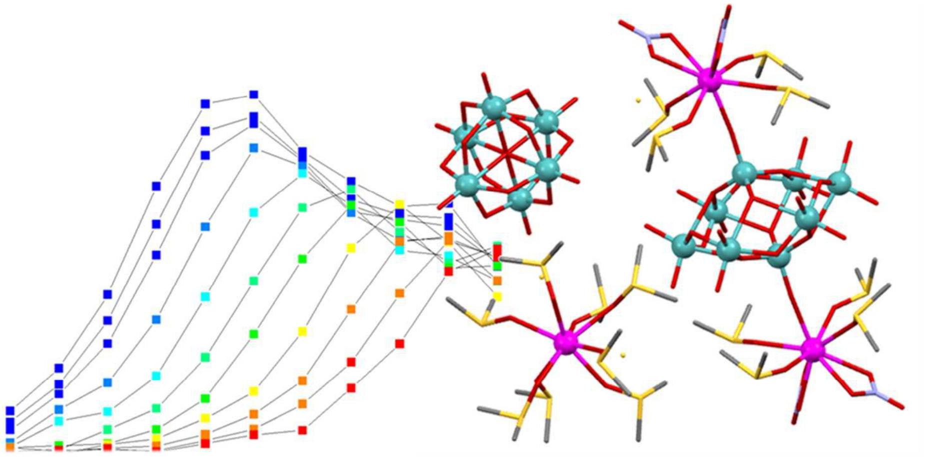

Journal Name

ARTICLE

Single-molecule magnet behaviour in polynuclear assembly of trivalent Cerium ions with Polyoxomolybdates

Received 00th January 20xx,
Accepted 00th January 20xx

DOI: 10.1039/x0xx00000x

www.rsc.org/

A. Ben Khélifa,[a] M. Salah Belkhiria,[a] G. Huang,[b] S. Freslon,[b] O. Guillou[b] and K. Bernot*

An isopolyoxomolybdate-based POM is coordinated to trivalent cerium ions to afford an hybrid complex namely, $[Ce(dmso)_8][Ce(\eta_2\text{-}NO_3)_2(dmso)_4(\alpha\text{-}Mo_8O_{26})_{0.5}][Mo_6O_{19}]$. The original electrostatic environment created around the Ce^{III} by its coordination to the isopolyoxomolybdate core induces a complex single-molecule magnet behavior.

Introduction

Polyoxometalates (POMs) constitute a large class of metal-oxygen oxo-clusters which are important candidates for the design and the synthesis of new hybrid organic-inorganic compounds. Their original structural features[1] induce remarkable physical properties. Indeed, POMs have a wide range of applications including catalysis[2], electronic semi-conductors[3], non-linear optics[4], biological and medical properties[5], magnetic properties[6], especially molecular magnetic properties.[7] In this regard, Dolbecq *et al.* reviewed a wide range of POMs and showed the relationship between POM structural properties and their applications areas.[8] The Mo-based Lindquist anions, $[Mo_6O_{19}]^{2-}$, are among the smallest members of the POMs family[9] and can be easily converted to octaoxomolybdate cluster $[Mo_8O_{26}]$.$^{4-}$[10,11] In this context, some hybrid materials based on hexaoxomolybdate anions $[Mo_6O_{19}]^{2-}$ and octaoxomolybdate anions $[Mo_8O_{26}]^{4-}$ have been employed as inorganic building blocks for the construction of supramolecular arrays with various organic ligands.[12,13]

The incorporation of lanthanide ions in polyoxometalates[14] is an important topic in the domain of supramolecular chemistry, because of their multiple coordination modes, their high oxophilic character and their multiple physical applications, such as magnetism[15], conductivity[16] or luminescence.[17-19] Such applications result from the synergy between the properties of the lanthanides ions and the POM units.[20] In this regard, many strategies have been explored to prepare and characterize lanthano-polyoxometalates derivatives presenting magnetic properties. It has been reported that lanthanide cations can link to POMs by terminal or bridging oxygen atoms to afford building blocks that can be interconnected by hydrogen bonds and Van der Waals interactions to provide original hybrid frameworks.[21] More specifically an effective strategy is to synthesize original POM species using vacant polyoxoanions as inorganic multidentate building blocks in order to integrate transition metal or lanthanide metal ions. This leads to diverse lacunar POMs with interesting magnetic properties.[15,21] Several investigations involving high-dimensional supramolecular assemblies based on lacunary Keggin[22], lacunary Wells-Dawson [23] and Anderson [24] polyoxoanions have also been reported.[15,21,25-28]

Incidentally, POM have been found to be an original way to obtain single-molecule magnets (SMM).[29] SMM are a class of molecules that present intriguing magnetic properties. Their nanometric size give rise to quantum effects on their magnetic properties[30] and SMMs are considered as promising candidates for the development of molecular spintronics[31,32] high-density magnetic memories and quantum computing devices.[33-35] Lanthanides-based SMM[36-40] are currently an emerging field as the strong magnetic anisotropy of lanthanides ions is an asset to create molecular nanomagnets. As a consequence, combination of POM and lanthanide ions has afforded nice example of SMMs. For instance, Aldamen *et al*[7] have reported the structure and magnetic properties of the sodium salt of the $[ErW_{10}O_{36}]^{9-}$ which shows an SMM behavior. Last, a particularly beautiful example of solvent influence on magnetic properties of Dy-based Polyoxotungstate has been reported.[41]

In the present work, polyoxomolybdate anions have been used as building blocks and associated with Ce^{III} ions. This affords the first SMM based on polyoxometalate–containing cerium complex.

Experimental

---

[a] *Laboratoire de Physico-chimie des Matériaux, Université de Monastir, Faculté des Sciences, Avenue de l'environnement, 5019 Monastir, Tunisia. E-mail : benkhelifaarbia@gmail.com*

[b] *INSA, UMR 6226, Institut des Sciences Chimiques de Rennes, 35708 Rennes, France. E-mail : Kevin.Bernot@insa-rennes.fr*

Electronic Supplementary Information (ESI) available: [CCDC 1047235, representation of the crystal structure, additional crystal data, powder X-ray patterns, additional magnetic data]. See DOI: 10.1039/x0xx00000x

Materials and General Methods.

All chemicals of reagent grade were purchased from commercial sources and used without further purification. The $[(C_4H_9)_4N]_2[Mo_6O_{19}]$ salt was synthesized as described by Hur *et al.*[42] EDS measurements were carried out with a Hitachi TM-1000, Tabletop Microscope version 02.11 (Hitachi High-Technologies, Corporation Tokyo Japan) with EDS analysis system (SwiftED-TM, Oxford Instruments Link INCA). The detector is a Silicon drift detector, with an energy resolution of 165eV which allows detecting the element from Na to U. The samples were assembled on carbon discs, stuck on an aluminum stub fixed at 7mm from EDX beam, with an angle of measurement of 22°. The Fourier transform infrared (FT-IR) spectra were recorded from KBr pellets in the range 4000-400 cm^{-1} on a Shimadzu FTIR-8400 spectrometer. X-ray powder patterns have been collected using a Panalytical X'Pert Pro diffractometer with an X' Celerator detector. The typical recording conditions were 40kV, 40mA for Cu-Kα (λ=1.542Å), the diffractograms were recorded in θ/θ mode in 60 min between 5° and 75° (8378 measurements) with a step size of 0.0084° and a scan time of 3600s. The calculated patterns were produced using Powdercell and WinPLOTR software programs.[43,44] Figure S1, presents experimental and simulated powder X-ray diffraction patterns for compound **1** that confirms the purity of the sample. Magnetic measurements were performed on pellets in order to avoid in-field crystallites orientation. Alternating and direct (ac and dc) magnetic measurements were performed with a MPMS Quantum Design SQUID magnetometer between 2 and 300 K. All measurements were corrected for the diamagnetic contribution of the sample and the sample holder.

Synthesis of $[Ce(dmso)_8][Ce(\eta_2\text{-}NO_3)_2(dmso)_4(\alpha\text{-}Mo_8O_{26})_{0.5}][Mo_6O_{19}]$ (1)

$[Ce(dmso)_8][Ce(\eta_2\text{-}NO_3)_2(dmso)_4(\alpha\text{-}Mo_8O_{26})_{0.5}][Mo_6O_{19}]$ (**1**) has been synthesized by mixing DMSO solutions of $Ce(NO_3)_3.6H_2O$ (1mmol; 0.433g) with $[(C_4H_9)_4N]_2[Mo_6O_{19}]$ (0.2 mmol; 0.273g). hexaoxomolybdate can be converted into to octaoxomolybdate polyoxoanion when heated.[45] In our case the mixture is heated under stirring at 333 K for 2 hours without any addition of acidic moieties. This later points are found to be particularly important as shortest heating time[14] and/or addition of phtalic acid[14] has been found to hamper the creation of the octaoxomolybdate moiety. The reaction solution is then allowed to slowly diffuse through 2-propanol. Yellow crystals of **1** were collected in 75 % yield based on Mo, from tube reactions.

Elemental Anal. Calcd (%) for C_{24} H_{72} Ce_2 Mo_{10} N_2 O_{50} S_{12} (2830.8): C 10.17, H 2.56, N 0.98; found 10.09, H 2.98, N 1.05 Ce, 9.96; Mo, 34.10 ; S, 13.68 %. EDS Mo/S ratio Calcd: 3.50 Found: 3.29. IR (cm^{-1}): 3013 (vw), 2914 (vw), 2850 (vw), 1630 (s), 1383 (w), 1010 (s), 960 (ep), 944 (s), 913(s), 840(s), 796 (w), 716 (s), 659 (w), 556 (w), 520 (w), 476 (vw), 438 (vw).

X-ray Crystallographic study

A single crystal of **1** was mounted on a Bruker- Nonius FR590 Kappa CCD single-crystal diffractometer equipped with graphite-monochromated Mo Kα radiation (λ = 0.71073Å) at 223(2) K. Data reduction and cell refinement were performed with Denzo and Scalepack programs.[46] The structure was solved by direct method using SIR-2004 program[47] and refined by full-matrix least-squares on Fo using the SHELXL-97 program.[48] The non-hydrogen atoms were refined anisotropically. Crystal data collection and refinement parameters of compound (**1**) are given in Table S1.

Results and discussion

Crystal Structure Description of $[Ce(dmso)_8][Ce(\eta_2\text{-}NO_3)_2(dmso)_4(\alpha\text{-}Mo_8O_{26})_{0.5}][Mo_6O_{19}]$

Structural analyses reveal that $[Ce(dmso)_8][Ce(\eta_2\text{-}NO_3)_2(dmso)_4(\alpha\text{-}Mo_8O_{26})_{0.5}][Mo_6O_{19}]$ crystallizes in the monoclinic system with P21/n space group (Table S1).

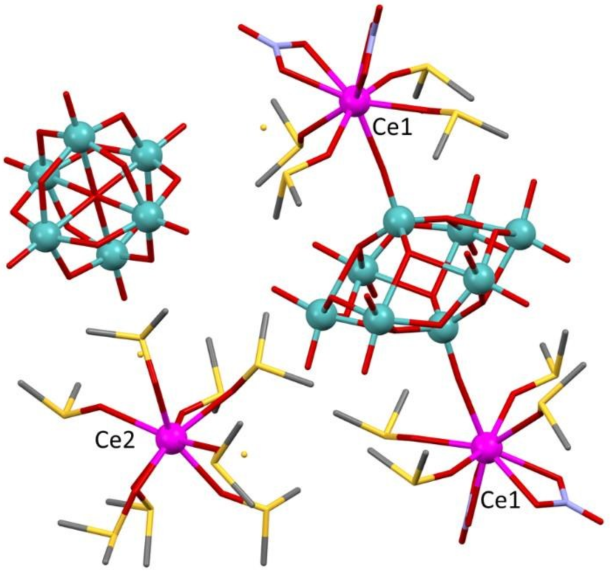

Figure 1. Representation of **1** with cerium atoms as purple balls and molybdenum atoms as green balls.

The asymmetric unit is made of one uncoordinated cationic complex $[Ce(dmso)_8]^{3+}$, one Lindqvist-type anion $[Mo_6O_{19}]^{2-}$ and one anionic molecular moiety $[Ce(\eta_2\text{-}NO_3)_2(dmso)_4(\alpha\text{-}Mo_8O_{26})_{0.5}]^{1-}$. Symmetry operations within the unit cell generate a $[(Ce(\eta_2\text{-}NO_3)_2(dmso)_4)_2(\alpha\text{-}Mo_8O_{26})_1]$ supramolecular compound where the $(\alpha\text{-}Mo_8O_{26})^{4-}$ POM, acts as a bidentate ligand and is coordinated to cationic cerium complex Ce1 through two terminal oxygen atoms. Each of the Ce1 is then nine-coordinated by four oxygen atoms from two nitrate molecules, four oxygen atoms from four dimethylsulfoxide molecules and one oxygen atom from $(\alpha\text{-}Mo_8O_{26})^{4-}$ (Figure 1). Continuous Shape Measurements (CSM)[49-51] highlight that Ce1 ions do not possess a well-defined symmetry of their surroundings (Table S2). The nine-coordinated atoms adopt a distorted spherical tricapped trigonal prism coordination environment (D3h site symmetry). On the contrary, Ce2 atoms are 8-coordinated, and clear biaugmented trigonal prism is observed (C2v symmetry) (Figure S2). The Ce–O bonds lengths are in the range 2.391(4) Å -2.653(4) Å (Table S3).

Going into details, the two Mo-based POMs adopt different topologies. The uncoordinated $[Mo_6O_{19}]^{2-}$ polyanion is a compact arrangement of six octahedra $[Mo_6]$ that share common edges and one common vertex. Three kinds of oxygen atoms are found, depending on their coordination in the moiety. A central oxygen atom O_c is hexacoordinated by all the molybdenum ions. Twelve double-bridging oxygen, $O_{(\mu 2)}$, link the Mo ions two by two. Finally each Mo ion is capped by a terminal oxygen O_t. Consequently, the Mo–O bond lengths fall into three classes: Mo–O_t bond lengths range from 1.672 (6) to 1.690 (4) Å, Mo-$O_{(\mu 2)}$ range from 1.901 (4) Å to 1.944 (4) Å, while Mo-O_c range from 2.305 (3) to 2.324 (3). On the other hand, the α-isomer of the octaoxomolybdate cluster $[\alpha\text{-}Mo_8O_{26}]^{4-}$ is made of six edge-sharing $[MoO_6]^{6-}$ octahedra that forms an equatorial ring with the poles capped by two $[MoO_4]^{2-}$ tetrahedra. As for the first Mo-based POM, the oxygen atoms within $[Mo_8O_{26}]$ could be divided into three sets, namely, terminal oxygen atoms O_t with Mo–O_t distances of 1.691(4) Å – 1.720(4) Å, double bridging oxygen atoms with Mo-$O_{(\mu 2)}$ distances of 1.885 (3) Å – 1.926(3) Å, and triple bridging oxygen atoms with Mo-$O_{(\mu 3)}$ 1.767(3) Å – 2.581(3) Å. All these Mo-O distances are in the range expected for the octahedrally coordinated Mo atoms of polyoxomolybdate clusters with small differences resulting from the distortion from the O_h geometry, in agreement with in literature.[52,53]

The crystal packing of **1** is made of layers of $[Mo_6O_{19}]^{2-}$ and $[(Ce(\eta^2\text{-}NO_3)_2(dmso)_4)_2(\alpha\text{-}Mo_8O_{26})]$ alternatively spaced in the (ac) plane (Figure S3) with the counter-cation $[Ce(dmso)_8]^{3+}$ regularly distributed in the interspaces. Supramolecular interactions tailor the 3D arrangement of all the moieties (Table S4).

Magnetic measurements

On the magnetic point of view, the two crystallographically different cerium atoms are expected to have very different behaviors. On one hand Ce1 atoms are part of trimeric entities in which two Ce1 ions are linked via the Mo-based POM that acts as a diamagnetic bridge. Even if metallic diamagnetic bridges are known to be able to transmit magnetic interactions,[54,55] the long Ce1-Ce1 distance (> 12 Å) may precludes the observation of such interactions. On the other hand, Ce2 atoms are uncoordinated and fully solvated moieties that are packed in between the trimers together with an additional and uncoordinated diamagnetic Mo-based POM.

Minute modification of the environment of magnetic molecules can strongly affect their magnetic behavior.[56,57] A feature that is also visible when molecule are grafted onto surfaces.[58,59] Trivalent lanthanides ions are probably the most affected[29,36,39,40,60,61] as their magnetic properties are strongly linked with the electrostatic distribution of their first or second coordination sphere.[62-67] For the particular case of the Ce^{III} ion, it belongs to the "oblate" lanthanides, *i.e.* ions for which the free-ion electronic density is "oblate" and consequently is stabilized by an axial crystal-field.[66] Such stabilization of the magnetic sublevels possibly induces magnetic slow relaxation and so single-molecule magnet behavior.

In the title compound, all Ce^{III} coordinating atoms are oxygens (Table S3). Ce2 atoms are 8-coordinated and all ligands atoms are dimethylsulfoxide molecules. It seems reasonable to anticipate that all coordinating oxygens generate a quite similar electrostatic potential. This picture is far from an asset for the stabilization of an oblate electronic density. On another hand, Ce1 atoms are nine-coordinated by oxygen atoms that belong to significantly different moieties and are not expected to generate an isotropic electrostatic potential on the lanthanide ions. Four oxygen atoms belong to negatively charged nitrate anions and cap Ce1 from one side. On the opposite side of the coordination polyhedron the oxygen atom of the POM moiety is likely to be charged because of the four negative charges of the POM. In the middle of these two extremes, neutral DMSO molecules complete the coordination sphere. On the electrostatic point of view, such geometry around the Ce^{III} is then close to a sandwich-type coordination that may be favorable for the observation of SMM behavior on oblate ions.[66]

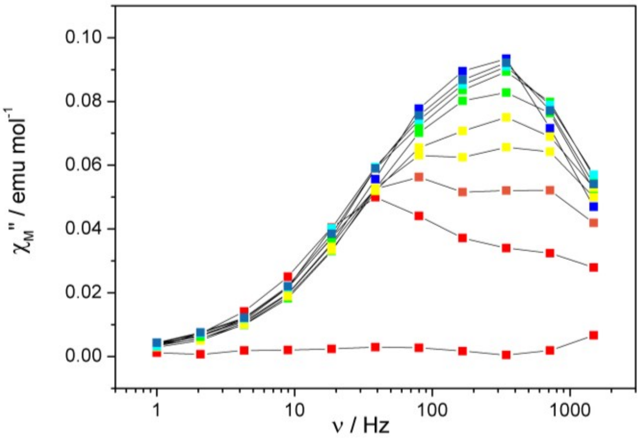

Figure2. Frequency dependence of the out-of-phase component of the magnetization of **1** measured from 0 Oe (red) to 1800 Oe (blue) with a 200 Oe step at 2K.

From the best of our knowledge, if anisotropy of molecules based-on Ce^{III} has already been observed and studied in details,[68,69] only two Ce^{III}-based single molecule-magnets are reported. The first one is a Zn^{II}-Ce^{III}-Zn^{II} trinuclear complex ("**Zn-Ce-Zn**") where the Ce^{III} ion is sandwiched by two phenoxo oxygen donors.[70] The second one is a mononuclear compound where a Ce^{III} ion is coordinated by two 1,4-bis(trimethylsilyl)-cyclooctatetra-enyldianion ("**CeCOT**") that thus also present a sandwich-like coordination.[71]

Static magnetic measurements have been conducted and as observed for **CeCOT**, the $\chi_M T$ value at 300K is significantly lower (1.25 emu.K.mol^{-1}) than the expected one for two Ce^{III} ions (1.6 emu.K.mol^{-1}). The $\chi_M T$ value decreases monotonically as the temperature is lowered (Figure S4). This is a consequence of the progressive depopulation of the Stark sub-levels as commonly seen on this kind of compounds. Such decrease is commonly simulated by considering appropriate crystal-field parameters.[72-76] However this procedure has not been applied here as the two drastically different crystal-fields around the two Ce^{III} ions would let to overparametrization of the monotonic decrease.

On the dynamic point of view, no ac signal is observed in zero field but a very small dc field (200 Oe) is enough to show magnetic slow relaxation as previously observed on **CeCOT** [71] (Figure 2 and S5).

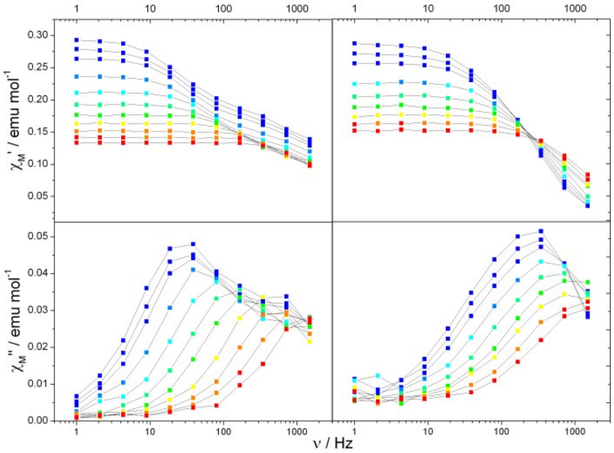

Figure 3. Frequency dependence of the in-phase (top) and out-of-phase component of the magnetization of **1** (bottom) measured with 200 Oe (left) and 1400 Oe dc field (right) from 1.8 K (blue) to 4 K (red).

On the basis of the structural and electrostatic considerations made above, one can assign this slow relaxation pathway (SR1) to Ce2. As observed on **CeCOT**, **1** also presents double-peaked χ_M" vs frequency curves below 3K (Figure 2 and S6). Another relaxation pathway (SR2) is then observed and attributed to Ce2. Cole-Cole plots[77] confirm this finding as low temperature fits were possible only if two relaxation times were considered (Figure 4 and S7). As a consequence, normalization of the plots over χ_T, the isothermal susceptibility, indicates that only part of the sample is relaxing according to each of these modes as χ_M' /χ_T is far from zero for SR1 and for SR2 (Table S5 and S7).

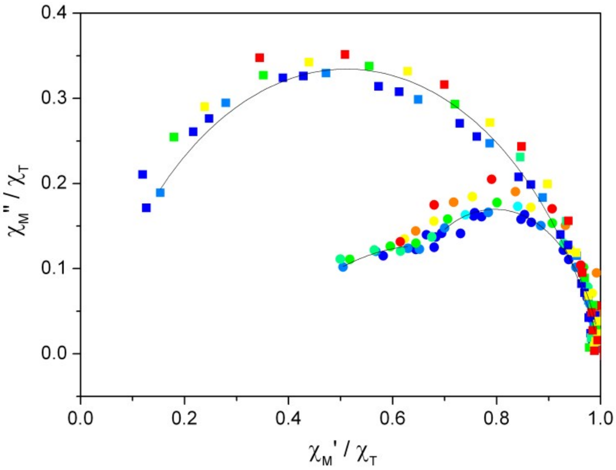

Figure 4. Normalized Cole-Cole diagrams of **1** between 1.8 K (blue) and 3.2K (red) in 200 Oe (circles) and 1400 Oe (squares) dc field. Lines represent the best fits at 2K as calculated with an extended Debye model.

As the static field is raised, another and fast relaxation (FR) pathway is seen for a dc field of 1400 Oe. It is not possible to unambiguously assess the origin of this relaxation mode and none of **CeCOT** and **Zn-Ce-Zn** have been investigated for such high dc field. However, only one peak in χ_M" *vs* frequency curves is observed together with almost zero χ_M' /χ_T values in Cole-Cole plots (Figure 4 and S7, Table S8). This tends to support the hypothesis of a contribution of a unique cerium center, probably Ce2. In fact, the unfavorable electrostatic coordination environment of Ce1 probably makes it silent on the dynamic point of view.

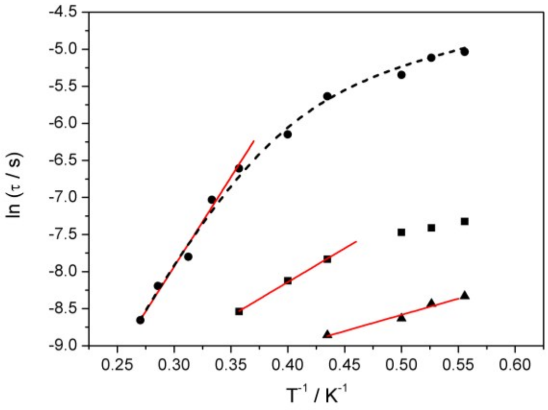

Figure 5. Relaxation time of **1** (τ) plotted against T^{-1} extracted from the 1400 Oe (squares) and 200 Oe measurements. For this last field the two different regimes are represented as circles (SR1) or triangles (SR2). The dashed line represents the best fit of SR1 regime considering Raman processes while the straight lines consider an Orbach process.

All three relaxation modes were tentatively analyzed considering a thermally activated (Orbach) magnetic relaxation (Figure 5). Energy barrier for spin reversal are 24.4 K, 4.4 K and 9.1 K with corresponding τ_0 values of 2.56 10^{-7}s, 2.09 10^{-5}s and 1.12 10^{-6}s for SR1, SR2 and FR respectively (Table S5 and S6). These values are closely comparable with the one of **CeCOT** and **Zn-Ce-Zn**. The curvature in the Arrhenius plots suggests a possible influence of direct or Raman processes.[61,65] In the present case very weak influence of direct process is observed. Reliable fitting of the relaxation time is obtained only on SR1 and a Raman process is identified with a variable exponent n=2 (with 27.12 K and 1.29 10^{-7} s).

Conclusions

As a conclusion we report here the first SMM based on polyoxometalate-containing cerium complex. This compound is made of an original Ce-POM-Ce trimer and one fully solvated Ce^{III} ion. It shows a complex single-molecule magnet behavior with almost three different relaxation pathways. By analogy with a previously reported compound the low field relaxation modes (SR1 and SR2) are attributed to Ce1, the cerium ions linked to the Mo-based POM. Another and faster regime (FR) is observed for higher field. In this compound the POM moiety is an asset as it permits the creation of original coordination environment for the lanthanide and so favors its magnetic slow relaxation. Moreover, one can anticipate that the peculiar redox properties of POMs maybe a useful way to permit the redox–switching of magnetic behavior of lanthanide-based SMM[41,78] on such family of compounds. Last, this class of compounds maybe a nice playground to investigate new kind of interaction between light and magnetic properties as recently reported.[79]

Acknowledgements

The Ministry of Higher Education and Scientific Research of Tunisia is acknowledged for financial support. T. Guizouarn is acknowledged for magnetic measurements.
Thanks are also expressed to the Pr. Michel Giorgi from the Université d'Aix-Marseille, Faculté des Sciences St-Jérôme for single-crystal crystallographic data collection.

Notes and references

1 D. L. Long, R. Tsunashima and L. Cronin, Angew. Chem., Int. Ed., 2010, **49**, 1736-1758.
2 D.-L. Long, E. Burkholder and L. Cronin, *Chem. Soc. Rev.* 2007, **36**, 105-121.
3 E. Coronado, C. Giménez-Saiz and C.J. Gómez-García, *Coord. Chem. Rev.* 2005, **249**, 1776-1796.
4 (a) C-G. Liu, W. Guan, L-K.Yan, Z-M. Su, P. Song and E-B.Wang, *J. Phys. Chem. C*, 2009, **113**, 19672-19676. (b) T. Zhang, L. Yan, S. Wen, S. Cong, J. Wang and Z. Su, *Molecular Simulation,* 2012, **38**, 518-524. (c) T. Zhang, L-K. Yan, S. Cong, W. Guan and Z-M.Su., *Inorg. Chem. Front.*, 2014, **1**, 65-70.
5 T. Yamase, *J. Mater. Chem.* 2005, **15**, 4773–4782.
6 R. Kitaura, S. Kitagawa, Y. Kubota, T.C. Kobayashi, K. Kindo, Y. Mita, S. Matsuo, M. Kobayashi, H.C. Chang, T.C. Ozawa, M. Suzuki, M. Sakata and M. Takata, *Science.* 2002, **298**, 2358-2361.
7 (a) M. A. AlDamen, J. M. Clemente-Juan, E. Coronado, C. Marti- Gastaldo and A. Gaita-Arino, *J. Am. Chem. Soc.* 2008, 130, 8874–8875. (b) M. A. Aldamen, S. Cardona- Serra, Juan M. Clemente-Juan, E. Coronado, A. Gaita-Arino, C. Marti-Gastaldo, F. Luis, and O. Montero, *Inorg. Chem.* 2009, **48**, 3467-3479.
8 A. Dolbecq, E. Dumas, C.-R. Mayer and P. Mialane, Chem. Rev. 2010, **110**, 6009–6048.
9 H. R. Allcock, E. C. Bissell and E. T. Shaw, *Inorg. Chem*. 1973, **12**, 2963–2968
10 K. Heussner, K. Peuntinger, N. Rockstroh, S. Rau and C. Streb, *Dalton Trans*, 2015, 44, 330-337.
11 Q. Li, P. Yin, L. Shi and Y. Wei, *Eur. J. Inorg. Chem*, 2009, **34**, 5227-5232.
12 Y. Shi, W. Yang, G. Xue, H. Hu and J. Wang, *J. Mol. Struct*. 2006, **784**, 244-248.
13 A. Proust, B. Matt, R. Villanneau, G. Guillemot, P.Gouzerh, and G. Izzet, *Chem. Soc. Rev.* 2012, **41**, 7605-7622.
14 A. Ben Khélifa, M. Giorgi, M-S. Belkhiria, Acta Cryst. 2012 E68, m938-m939
15 X. Zhang, D.Wang, J. Dou, S. Yang, X. Yao and J. Jiang, *Inorg. Chem*. 2006, **45**, 10629-10635.
16 Y. P. Wang, B. B. Zhou and L. Y. Liu, *J. Alloys Comp.* 2008, **463**, 333-337.
17 C. L. Hill (guest ed.), *Chem. Rev.* 1998, **98**,1–390.
18 R. C. Howell, F. G. Perez, S. Jain, W. D. Horrocks Jr., A. L. Rheingold and L. C. Francesconi, *Angew. Chem. Int. Ed.* 2001, **40**, 4031-4034.
19 X. Wang, Y. Guo, Y. Li, E. Wang, C. Hu and N. Hu, *Inorg. Chem.* 2003, **42**, 4135-4140
20 S. Bareyt, S. Piligkos, B. Hasenknopf, P. Gouzerh, E. Lacote, S. Thorimbert and M. Malacria, *Angew. Chem. Int. Ed.* 2003, **42**, 3404-3406.
21 H. An, Z. Han and T. Xu, *Inorg. Chem.* 2010, **49**, 11403-11414.
22 J.-C. P. Gabriel, R. Nagarajan, S. Natarajan, A. K. Cheetham, and C. N. R. Rao, *J. Solid State Chem*. 1997,**129**, 257-262.
23 S. Bareyt, S. Piligkos, B. Hasenknopf, P. Gouzerh, E. Lacote, S. Thorimbert and M. Malacria, *Angew. Chem. Int. Ed.* 2003, **42**, 3404-3406.
24 B. Gao, S.X. Liu, L.H. Xie, M. Yu, Ch. D. Zhang, C.Y. Sun and H.Y. Cheng, *J. Solid State Chem.* 2006, **179**, 1681-1689.
25 Q. Tang, S-X. Liu, D-D. Liang, F-J. Ma, G-J. Ren, F. Wei, Y. Yang and C-C. Li, *J. Solid State Chem*, 2012, **190**, 85-91.
26 J-Y. Niu, M-L. Wei and J-P. Wang, *J. Molstruct,* 2004, **689**, 147-152.
27 D. Drewes, E-M. Limanski and B. Krebs, *Dalton Trans*, 2004,**14**, 2087-2091.
28 C-D. Wu, C-Z. Lu, H-H. Zhuang and J-S. Huang, *J. Am. Chem. Soc,* 2002, **124**, 3836-3837.
29 C. Benelli and D. Gatteschi, *Introduction to Molecular Magnetism: From Transition Metals to Lanthanides*, 2015.
30 D. Gatteschi, R. Sessoli and J. Villain, *Molecular Nanomagnets* Oxford University Press: Oxford, 2006.
31 L. Bogani and W. Wernsdorfer, *Nat. Mater*. 2008, 7, 179-186.
32 S. Sanvito, *Chem. Soc. Rev.* 2011, **40**, 3336-3355.
33 M. N. Leuenberger and D. Loss. *Nature,* 2001, **410**, 789-793.
34 F. Troiani and M. Affronte, *Chem. Soc. Rev.* 2011, **40**, 3119-3129.
35 G. Aromí, F. Luis and O. Roubeau, *In Lanthanides and Actinides in Molecular Magnetism; Wiley- VCH Verlag GmbH & Co. KGaA*: 2015, p 185-222.
36 P. Zhang, L. Zhang and J. Tang *Dalton Trans.* 2015, **44,** 3923-3929.
37 R. Sessoli and K. Bernot, In *Lanthanides and Actinides in Molecular Magnetism*; Wiley-VCH Verlag GmbH and Co. KGaA: 2015, p 89-124.
38 J. Tang and P. Zhang, In *Lanthanides and Actinides in Molecular Magnetism*; Wiley-VCH Verlag GmbH and Co. KGaA: 2015, p 61-88.
39 H. L. C.Feltham and S. Brooker *Coord. Chem. Rev.* 2014, **276**, 1-33.
40 D. N. Woodruff, R. E. P. Winpenny and R. A. Layfield *Chem. Rev.* 2013, **113**, 5110-5148.
41 K. Suzuki, R. Sato and N. Mizuno, *Chem. Sci.* 2013, **4**, 596-600.
42 N. H. Hur, W. G. Klemperer and R.-C. Wang, *Inorg. Synth.* 1990, **27**, 77-78.
43 W. Kraus and G. Nolze, *J. Appl. Cryst.* 1996, **29**, 301-303.
44 T. Roisnel and J. Rodriguez-Carvajal: WinPLOTR: a window tool for powder diffraction pattern analysis. Materials Science Forum, Proceedings of the Seventh European Powder Diffraction Conference (EPDIC 7), Ed. R. Delhez and E.J. Mittenmeijer 2001, **378**, 118-123.
45 W. G. Klemperer and W. Shum, *J. Am. Chem. Soc.* 1976, **98**, 8291-8293.
46 G. M. Sheldrick, *ActaCryst. A* 2008, **64**, 112-122.
47 Z. Otwinowski and W. Minor, Methods in Enzymology. 1997, **276**, 307–326. *Macromolecular Crystallography*, part A, edited by C.W. Carter Jr. & R. M. Sweet. New York: Academic Press.
48 M. C. Burla, R. Caliandro, M. Camalli, B. Carrozzini, G. L. Cascarano, L. De Caro, C. Giacovazzo, G. Polidori, and R. Spagna, *J. Appl. Cryst*. 2005, **38**, 381–388.
49 S. Alvarez, P. Alemany, D. Casanova, J. Cirera, M. Llunell and D. Avnir, *Coord. Chem. Rev.* 2005,**249**, 1693-1708.

50 D. Casanova, J. Cirera, M. Llunell, P. Alemany, D. Avnir and S. Alvarez, *J. Am. Chem. Soc.* 2004, **126**, 1755-1763.

51 S. Alvarez, D. Avnir, M. Llunell and M. Pinsky, *New J. Chem*.2002, **26**, 996-1009.

52 B. K. Koo and U. Lee, *Inorg. Chim. Acta,* 2006, **359**, 2067-2071

53 (a) R. S. Rarig Jr and J. Zubieta, *Polyhedron.* 2003, **22**, 177-188; (b) Y. YinNiu, L.F. Wang, X.R. Lv, H.J. Du, Y.Z. Qiao, H.M. Wang, L.S. Song, B.L. Wu, H.W. Houa and S.W. Ngb. *CrystEng Comm*. 2011, **13**, 5071-5081.

54 F. Pointillart, K. Bernot, R. Sessoli and D. Gatteschi, *Inorg. Chem.* 2010, **49**, 4355-4361.

55 K. Bernot, J. Luzon, L. Bogani, M. Etienne, C. Sangregorio, M. Shanmugam, A. Caneschi, R. Sessoli and D. Gatteschi, *J. Am. Chem. Soc.* 2009, **131**, 5573-5579.

56 M. Mannini, F. Bertani, C. Tudisco, L. Malavolti, L. Poggini, K. Misztal, D. Menozzi, A. Motta, E. Otero, P. Ohresser, P. Sainctavit, G. G. Condorelli, E. Dalcanale and R. Sessoli, *Nat Commun*, 2014, **5**.

57 G. Cucinotta, M. Perfetti, J. Luzon, M. Etienne, P.-E. Car, A. Caneschi, G. Calvez, K. Bernot and R. Sessoli, *Angew. Chem. Int. Ed.*, 2012, **51**, 1606-1610.

58 M. Mannini, F. Pineider, C. Danieli, F. Totti, L. Sorace, P. Sainctavit, M. A. Arrio, E. Otero, L. Joly, J. C. Cezar, A. Cornia and R. Sessoli, *Nature*, 2010, **468**, 417-421.

59 M. Mannini, F. Pineider, P. Sainctavit, C. Danieli, E. Otero, C. Sciancalepore, A. M. Talarico, M. A. Arrio, A. Cornia, D. Gatteschi and R. Sessoli, *Nat. Mater.*, 2009, **8**, 194-197.

60 *Lanthanides and Actinides in Molecular Magnetism*; Ed. Layfield R.A. and Mueugesu M., Wiley-VCH Verlag GmbH & Co. KGaA: 2015.

61 L. Sorace and D. Gatteschi, In *Lanthanides and Actinides in Molecular Magnetism*; Wiley-VCH Verlag GmbH & Co. KGaA: 2015, p 1-26.

62 J. Jung, F. Le Natur, O. Cador, F. Pointillart, G. Calvez, C. Daiguebonne, O. Guillou, T. Guizouarn, B. Le Guennic and K. Bernot, *Chem. Commun.* 2014, **50**, 13346-13348.

63 J. Jung, O. Cador, K. Bernot, F. Pointillart, J. Luzon and B. Le Guennic, *Beilstein J. Nano.* 2014, **5**, 2267-2274.

64 F. Pointillart, K. Bernot, S. Golhen, B. Le Guennic, T. Guizouarn, L. Ouahab and O. Cador, *Angew. Chem. Int. Ed.* 2015, **54**, 1504-1507.

65 L. Ungur, J. J. Le Roy, I. Korobkov, M. Murugesu and L. Chibotaru, *Angew. Chem. Int. Ed.* 2014, **53**, 4413-4417.

66 J. D. Rinehart and J.R. Long, *Chem. Sci.* 2011, **2**, 2078-2085.

67 S. Gómez-Coca, D. Aravena, R. Morales and E. Ruiz, *Coord. Chem. Rev.* 2015, **289–290**, 379-392.

68 L. Sorace, C. Benelli and D.Gatteschi, *Chem. Soc. Rev.* 2011, **40**, 3092-3104.

69 L. Sorace, C. Sangregorio, A. Figuerola, C. Benelli and D.Gatteschi, *Chem. Eur. J.* 2009, **15**, 1377-1388.

70 S. Hino, M. Maeda, K. Yamashita, Y. Kataoka, M. Nakano, T. Yamamura, H. Nojiri, M. Kofu, O. Yamamuro and T. Kajiwara, *Dalton Trans.* 2013, **42**, 2683-2686.

71 J. J. Le Roy, I. Korobkov, J. E. Kim, E. J. Schelter and M. Murugesu, *Dalton Trans.* 2014, **43**, 2737-2740.

72 X. Yi, K. Bernot, V. Le Corre, G. Calvez, F. Pointillart, O. Cador, B. Le Guennic, J. Jung, O. Maury, V. Placide, Y. Guyot, T. Roisnel, C. Daiguebonne and O. Guillou, *Chem. Eur. J.* 2014, **20**, 1569-1576.

73 M. Perfetti, E. Lucaccini, L. Sorace, J. P. Costes and R. Sessoli, *Inorg. Chem.* 2015, **54**, 3090-3092

74 E. Lucaccini, L. Sorace, M. Perfetti, J. P. Costes and R. Sessoli, *Chem. Commun.* 2014, **50**, 1648-1651.

75 F. Pointillart, B. Le Guennic, S. Golhen, O. Cador, O. Maury and L. Ouahab, *Chem. Commun.* 2013, **49**, 615-617.

76 J. M. Clemente-Juan, E. Coronado and A.Gaita-Ariño, In *Lanthanides and Actinides in Molecular Magnetism*; Wiley-VCH Verlag GmbH & Co. KGaA: 2015, p 27-60.

77 K. S. Cole and R. H. Cole, *J. Chem. Phys.* 1941, **9**, 341-351.

78 L. Norel, M. Feng, K. Bernot, T. Roisnel, T. Guizouarn, K. Costuas and S. Rigaut, *Inorg. Chem.* 2014, **53**, 2361-2363.

79 R. Sessoli, M.-E. Boulon, A. Caneschi, M. Mannini, L. Poggini, F. Wilhelm and A. Rogalev, *Nat. Phys.*, 2015, **11**, 69-74.